# Identification and Mitigation of a Reactive Metabolite Liability Associated with Aminoimidazoles

**ARTICLE** *in* CHEMICAL RESEARCH IN TOXICOLOGY · AUGUST 2014

Impact Factor: 3.53 · DOI: 10.1021/tx500212c · Source: PubMed



**5 AUTHORS**, INCLUDING:

Sreekanth Ramachandran
Integral Biosciences
**22** PUBLICATIONS **1,197** CITATIONS
SEE PROFILE

Shahul Hameed P
Bugworks Research India Pvt Ltd, Bangalore, i…
**19** PUBLICATIONS **124** CITATIONS
SEE PROFILE

Vijaykamal Ahuja
AstraZeneca
**8** PUBLICATIONS **67** CITATIONS
SEE PROFILE

Vinayak Hosagrahara
AstraZeneca
**32** PUBLICATIONS **671** CITATIONS
SEE PROFILE

Chemical Research in Toxicology

Article

pubs.acs.org/crt

# Identification and Mitigation of a Reactive Metabolite Liability Associated with Aminoimidazoles

Abhishek Srivastava,[†] Sreekanth Ramachandran,[‡] Shahul P. Hameed,[‡] VijayKamal Ahuja,[†] and Vinayak P. Hosagrahara*[,§]

[†]Drug Metabolism and Pharmacokinetics, Infection IMED, and [‡]Department of Medicinal Chemistry, Infection IMED, AstraZeneca India Pvt. Ltd., Bangalore, India

[§]Drug Metabolism and Pharmacokinetics, Infection IMED, AstraZeneca, 35 Gatehouse Drive, Waltham, Massachusetts 02451, United States

Supporting Information

**ABSTRACT:** Reactive metabolites (RMs) have been implicated as causal factors in many drug-associated idiosyncratic toxicities. This study aims at identification and mitigation of an RM liability associated with aminoimidazole and amino(aza)-benzimidazole structural motifs from an antimalarial project. Nineteen compounds with different structural modifications were studied in rat and human liver microsomes using glutathione (GSH) and *N*-acetyl cysteine (NAC) as trapping agents for RM. Metabolite profiling of aminoimidazole compounds in initial studies revealed the presence of dihydrodiol metabolites suggestive of reactive epoxide precursors, confirmed by the identification of a dihydrohydroxy GSH conjugate in GSH supplemented incubations. Substitution of methyl group at a potential site of metabolism blocked the epoxidation; however, formation of an imine-methide RM was suspected. Masking the site of metabolism via benzimidazole and 4/7-azabenzimidazole resulted in the possible formation of quinone-imine intermediates as a product of bioactivation. Further, substitutions with electron withdrawing groups and steric crowding did not address this liability. Mitigation of bioactivation was achieved with 5/6-azabenzimidazole and with $CF_3$ substitution at the 6-position of the 7-azabenzimidazole ring. Moreover, compounds devoid of imidazole -$NH_2$ do not undergo bioactivation. This study, therefore, establishes aminoimidazole and amino(aza)benzimidazoles as potential toxicophores and describes ways to mitigate this bioactivation liability by chemical modification.

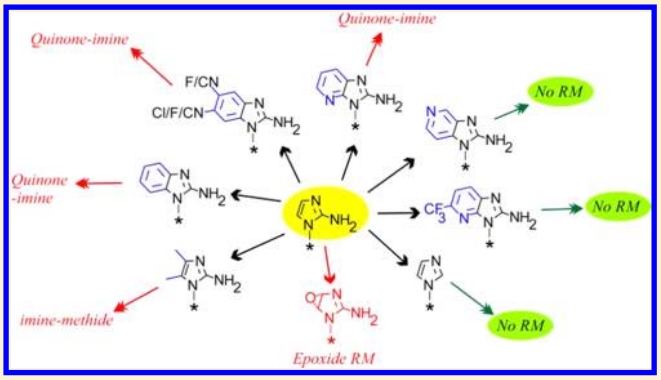


## INTRODUCTION

Idiosyncratic drug reactions represent a major problem for the pharmaceutical industry because they add significant uncertainty to the process of drug development and can lead to candidate failure.[1,2] It is believed that some idiosyncratic reactions are initiated by reactive drug metabolites,[3,4] which bind covalently to macromolecules and either cause direct cell damage or trigger an immune response leading to cell death.[5−7] Therefore, the propensity of a new chemical entity to undergo bioactivation needs to be determined at an early stage of the drug discovery process. Mitigation of this liability by removing the chemical alerts as early as possible can eliminate perceived reactive metabolite-mediated chemical liabilities and the need for extensive safety evaluation beyond standard practices.[8,9]

Nitrogen containing aromatic heterocycles, including imidazoles are of great medicinal chemistry interest. Owing to its polar and ionizable characteristics, the imidazole ring improves pharmacokinetic characteristics of molecules and thus is used as a remedy to optimize the solubility and bioavailability parameters of poorly soluble compounds.[10] A wide range of pharmacological active compounds including antibacterial, anticancer, antitubercular, antifungal, analgesic, and anti-HIV agents contain imidazole and/or benzimidazole motifs as part of their structure.[10−12]

In this article, we present a comprehensive study aiming at identification and mitigation of reactive metabolite (RM) liability associated with aminoimidazole and amino(aza)-benzimidazole structural motifs in a series of compounds from an antimalarial project. Initial lead molecules from this series showed the propensity to form reactive intermediates when incubated with human (HLMs) and rat liver microsomes (RLMs). Following structural modifications to mitigate this issue, several analogues were tested, and analogues devoid of the potential to form RMs were advanced for further testing as antimalarial agents. We also present potential bioactivation mechanisms for the initial leads and selected molecules.

**Received:** May 28, 2014

   dx.doi.org/10.1021/tx500212c | *Chem. Res. Toxicol.* XXXX, XXX, XXX−XXX

**Table 1. Identification and Characterization of Metabolites of Compounds 1 to 11, 13, and 16**

| Structure | Peak (m/z) | Key Fragments |
|---|---|---|
| 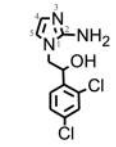 **Compound 1** m/z 272 | Parent (272) | 57, 84 |
| | Dihydrodiol metabolite (306) | 57, 117 |
| | NAC adducts (451)[b] | |
| | GSH Adducts (595)[b] | |
| 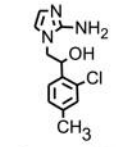 **Compound 2** m/z 252 | Parent (252) | 57, 84 |
| | Dihydrodiol metabolite (286) | 57, 117 |
| | NAC adducts (431)[b] | |
| | GSH Adducts (575)[b] | |
| 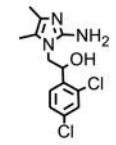 **Compound 3** m/z 300 | Parent (300) | 112 |
| | Hydroxy metabolite (316) | 110, 298 |
| | NAC Adduct (461) | 110, 298, 332[a] |
| | GSH adduct (605) | 298 |
| 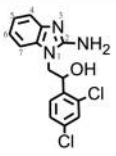 **Compound 4** m/z 322 | Parent (322) | 92, 134 |
| | Hydroxy metabolite (338) | 108, 150 |
| | NAC Adduct (499) | 182, 370[a] |
| | GSH adduct (643) | 370, 514 |
| 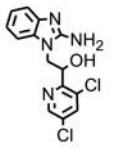 **Compound 5** m/z 323 | Parent (323) | 134, 189 |
| | Hydroxy Meabolite (339) | 150, 189 |
| | NAC adduct (500) | 182, 371[a] |
| | GSH Adduct (644) | 371 |
| 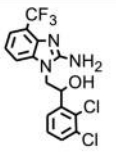 **Compound 6** m/z 390 | Parent (390) | 182 |
| | Hydroxy metabolite (406) | 198 |
| | NAC adduct (567) | 230, 438[a] |
| | GSH Adduct (711) | 230, 438, 582 |
| 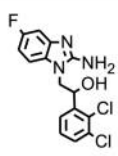 **Compound 7** m/z 340 | Parent (340) | 152 |
| | Hydroxy metabolite (356) | 168 |
| | NAC adduct (499) | 182, 370[a] |
| | GSH adduct (643) | 370 |

| Structure | Peak | Key Fragments |
|---|---|---|
| 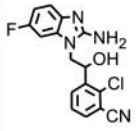 **Compound 8** m/z 331 | Parent (331) | 110, 152 |
| | Oxidativ defluorination (329) | 108, 150 |
| | NAC adduct (490) | 182, 361[a] |
| | GSH Adduct (634) | 361 |
| 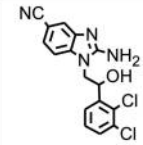 **Compound 9** m/z 347 | Parent (347) | 144, 159 |
| | Hydroxy met. (363) | 160, 175 |
| | NAC adduct (524) | 207, 395[a] |
| | GSH Adduct (668) | 395, 539 |
| 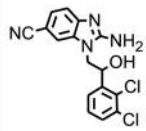 **Compound 10** m/z 347 | Parent (347) | 144, 159 |
| | oxidative denitri-lation (m/z 338) | 135, 150 |
| | NAC adduct (499) | 167, 182, 370[a] |
| | GSH Adduct (643)[b] | |
|  **Compound 11** m/z 374 | Parent (374) | 151, 186 |
| | Oxidativ defluorination (372) | 149, 184 |
| | NAC adduct (499) | 149, 182, 370[a] |
| | GSH Adduct (643)[b] | |
| 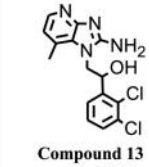 **Compound 13** m/z 337 | Parent (337) | 149 |
| | Hydroxy met. (353) | 165 |
| | NAC adduct (514) | 197, 385[a] |
| | GSH Adduct (658) | 197, 385, 529 |
| 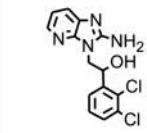 **Compound 16** m/z 323 | Parent (323) | 135 |
| | Hydroxy met. (339) | 151 |
| | NAC adduct (500) | 183, 371[a] |
| | GSH Adduct (644) | 183, 371, 515 |

[a] Fragment corresponding to NL 129 from NAC conjugate.
[b] Fragmentation profile of the metabolite could not be obtained.

## MATERIALS AND METHODS

**Chemicals.** Pooled HLMs (150 donors; equal gender mix) were obtained from BD Biosciences (Singapore). RLMs were prepared in-house as described earlier.[13] Reduced L-glutathione (GSH), β-nicotinamide adenine dinucleotide 2′-phosphate reduced tetrasodium salt (β-NADPH), formic acid (ultrapure), *N*-acetyl cysteine (NAC), dimethyl sulfoxide, and 1-aminobenzotriazole (ABT) were purchased from Sigma-Aldrich (Bangalore, India). All proprietary compounds (**1**−**19**) used in this article were synthesized internally at AstraZeneca, India. Methanol, water, and acetonitrile (ACN) were of HPLC grade and obtained from J.T. Baker, India. All other solvents were of HPLC


dx.doi.org/10.1021/tx500212c | *Chem. Res. Toxicol.* XXXX, XXX, XXX−XXX

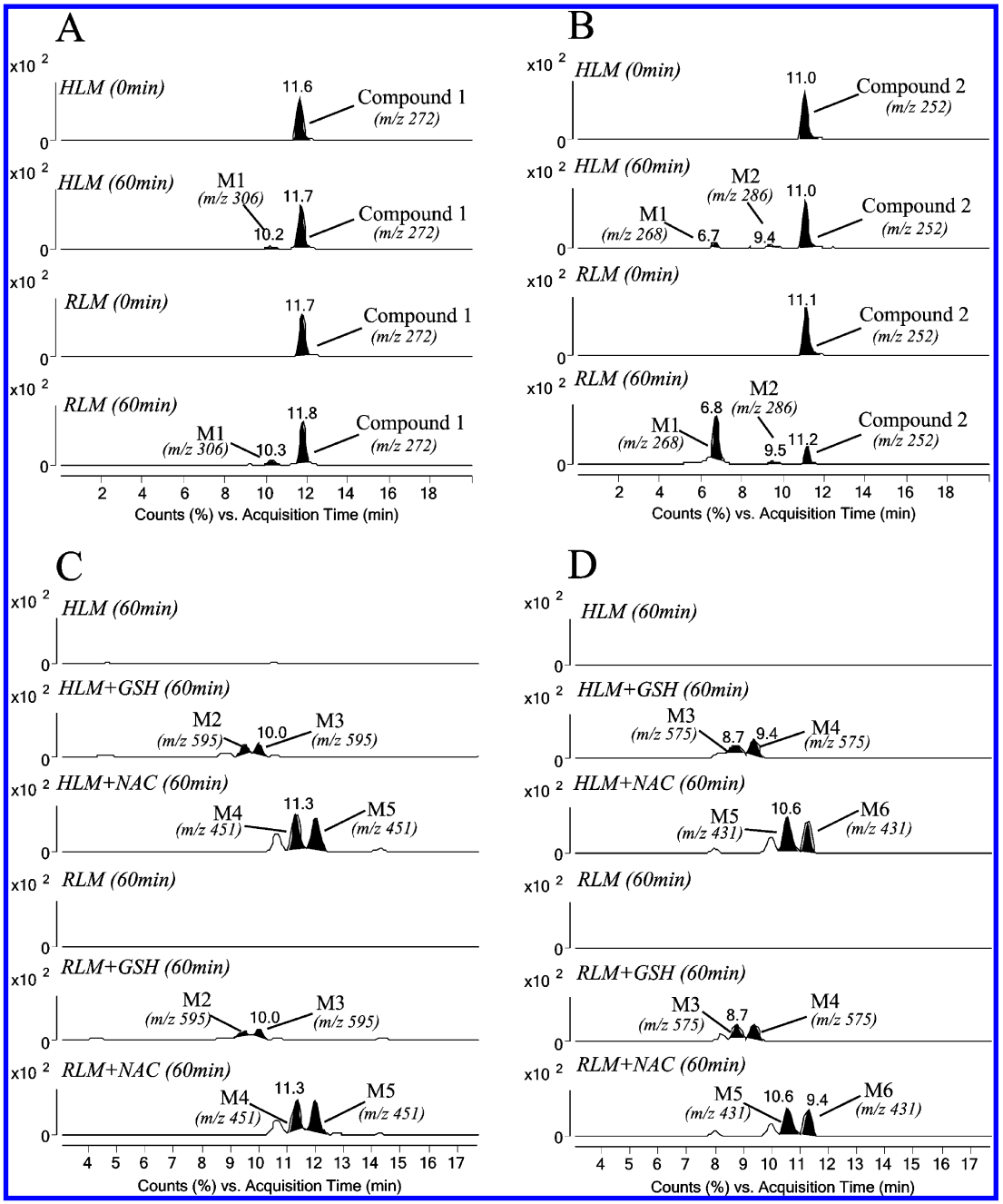


**Figure 1.** LC-MS base peak ion chromatograms (BPC) for the parent and metabolites. (A) Metabolism of **1** in HLM and RLM, and analysis of samples for BPC of $m/z$ 272 and 306. (B) Metabolism of **2** in HLM and RLM, and analysis of samples for BPC of $m/z$ 252, 268, and 286. (C) RM trapping with GSH and NAC for **1** in HLM and RLM, and analysis of samples for BPC of $m/z$ 595 and 451. (D) RM trapping with GSH and NAC for **2** in HLM and RLM, and analysis of samples for BPC of $m/z$ 575 and 431.

grade, and unless otherwise specified, all of the other reagents were purchased from Sigma-Aldrich.

***In Vitro* Incubations for the Reactive Metabolite Screen.** Each compound was incubated at a concentration of 10 $\mu$M with HLM/RLM (1 mg/mL protein) in 100 mM phosphate buffer (pH 7.4) in the presence of NADPH (2 mM). In parallel, compounds were also incubated with microsomes supplemented with either GSH (2 mM) or NAC (2 mM) as trapping agents to test for the formation of reactive metabolites. Incubations were performed for 60 min ($t_{60}$) in a shaking incubator at 37 °C. The microsomal reaction was terminated by the addition of an equal volume of ice-cold ACN, vortexed, and centrifuged at 13000 rpm for 10 min. The supernatant was collected for HPLC-UV/MS analysis. Control incubation samples were quenched at time = 0 ($t_0$) (prior to the addition of NADPH) with an equal volume of ice-cold ACN.

To establish the role of cytochrome P450 enzymes in the bioactivation of the amino-imidazole moiety, incubation of **1** and **2** (10 $\mu$M) was also carried out with aminobenzotriazole (ABT; 1 mM). For these incubations, ABT, microsomes, NADPH, and GSH or NAC were preincubated for 15 min before the addition of compound and supplementary NADPH (final concentration, 2 mM).

**LC-MS/MS Analysis.** An Agilent 1200 series HPLC system consisting of an autosampler, vacuum degasser, binary pump system, column oven, and PDA detector was used to monitor the formation of metabolites in microsomal samples. Metabolites were resolved with a Phenomenex Gemini C18 column (25 × 0.46 cm, 5-$\mu$m particle size). The mobile phase consisted of a combination of ACN containing


dx.doi.org/10.1021/tx500212c | *Chem. Res. Toxicol.* XXXX, XXX, XXX−XXX

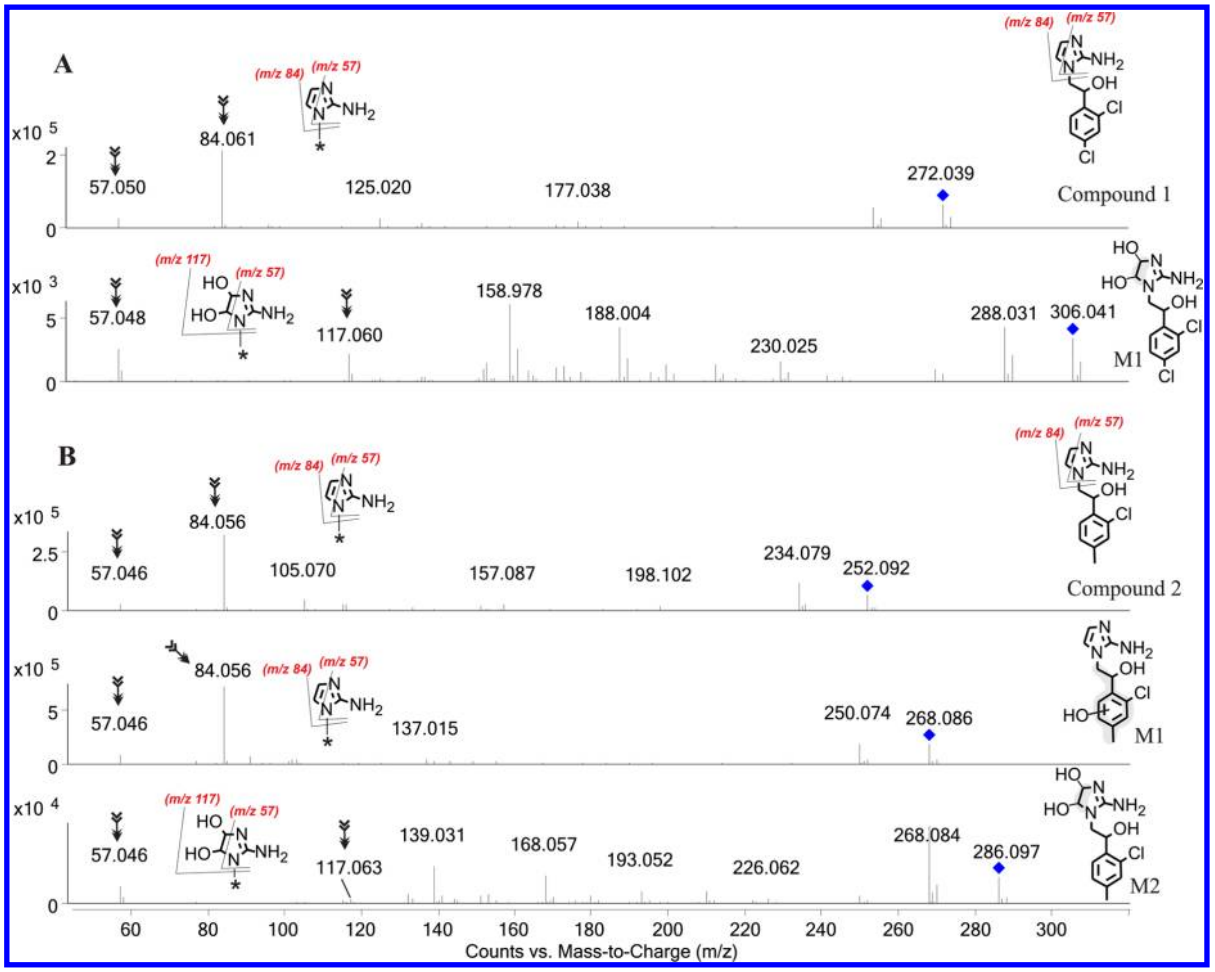


**Figure 2.** MS2 spectra of (A) **1** and metabolite, and (B) **2** and metabolites.

formic acid (0.05%, v/v) and 10 mM ammonium formate buffer. A sample aliquot of 40 $\mu$L was injected onto the column and eluted at 1 mL/min with a gradient maintained at 5% ACN for 5 min. The organic component was increased from 5% to 50% ACN between 5 to 20 min, maintained at 50% ACN for an additional 5 min, and finally returned to 5% ACN over 5 min. UV absorbance data were collected for a scan range of 220−320 nm with an in-line Agilent PDA detector. The HPLC eluent was directly coupled to an Agilent 6520 Q-TOF mass spectrometer with 500 $\mu$L/min eluate split-flow to the LC-MS interface. The instrument was operated in electrospray ionization (ESI) mode with positive polarity. Nitrogen was used as collision gas. Capillary voltage was +4000 V. Drying gas (nitrogen) was set at 350 °C with a flow rate of 13 L/min. Mass analysis was performed in auto-MS/MS mode with a mass range ($m/z$) of 100−800 in full scan and a mass range of ($m/z$) 40−800 in MS/MS mode.

## RESULTS

**Identification and Confirmation of RM Liability Associated with Amino-Imidazoles.** Metabolites of **1** (Table 1; $m/z$, 272 $[M + H]^+$) and **2** (Table 1; $m/z$, 252 $[M + H]^+$) were identified in RLM and HLM incubations by comparing 60 min incubation samples with control (0 min) incubations by using LC-MS (Figure 1A and B). Compound **1** underwent metabolism to form one metabolite (M1); whereas two metabolites M1 and M2 were observed for **2**. In LC-MS analysis, M1 (**1**) yielded a peak at $m/z$ 306 $[M + H]^+$ (Figure 1A), which is an addition of 34 Da to the parent at $m/z$ 272 $[M + H]^+$. The chemical formula derived from high-resolution MS (HRMS) data for M1 indicated the addition of two hydrogen and two oxygen atoms to the parent. Following hydrogen−deuterium exchange mass spectrometry analysis (HDMS), M1 exhibited an ion with $m/z$ 312 $[M + D]^+$, whereas its parent compound 1 revealed a peak at $m/z$ 276 $[M + D]^+$ (Figure S1.B, Supporting Information). Since **1** has 3 exchangeable protons, the mass of M1 corresponds to the addition of 2 exchangeable protons to the parent. On the basis of these observations, M1 (**1**) was tentatively characterized as the dihydrodiol metabolite. MS2 spectra of this metabolite (Figure 2A) suggested that the metabolism occurred on the imidazole ring of **1** at C4 and C5.

Two metabolites (M1 and M2) of **2** ($m/z$ 252 $[M + H]^+$) produced ion peaks at $m/z$ 268 $[M + H]^+$ (parent+16 Da) and $m/z$ 286 $[M + H]^+$ (parent+34 Da), respectively (Figure 1B). In the HDMS experiment, **2** had a peak at $m/z$ 256 $[M + D]^+$ (Figure S2.B, Supporting Information), while metabolites M1 and M2 produced peaks at $m/z$ 273$[M + D]^+$ and $m/z$ 292 $[M + D]^+$, respectively, indicating the addition of one exchangeable proton for M1 and two exchangeable protons for M2. MS2 spectra of M1 suggested hydroxylation at the lower part (chloro-methyl phenyl ring) of the molecule (Figure 2B) since the characteristic aminoimidazole fragment at $m/z$ 84 was intact. M2 (Figure 2B) was characterized as the dihydrodiol metabolite on the imidazole ring at C4 and C5 similar to the dihydrodiol metabolite (M1; Figure 2A) of **1**.

Compounds **1** and **2** were incubated with RLMs/HLMs fortified with NADPH in the presence and absence of GSH or NAC, and as shown in Figure 1C, two ion peaks (M2 and M3)


dx.doi.org/10.1021/tx500212c | Chem. Res. Toxicol. XXXX, XXX, XXX−XXX

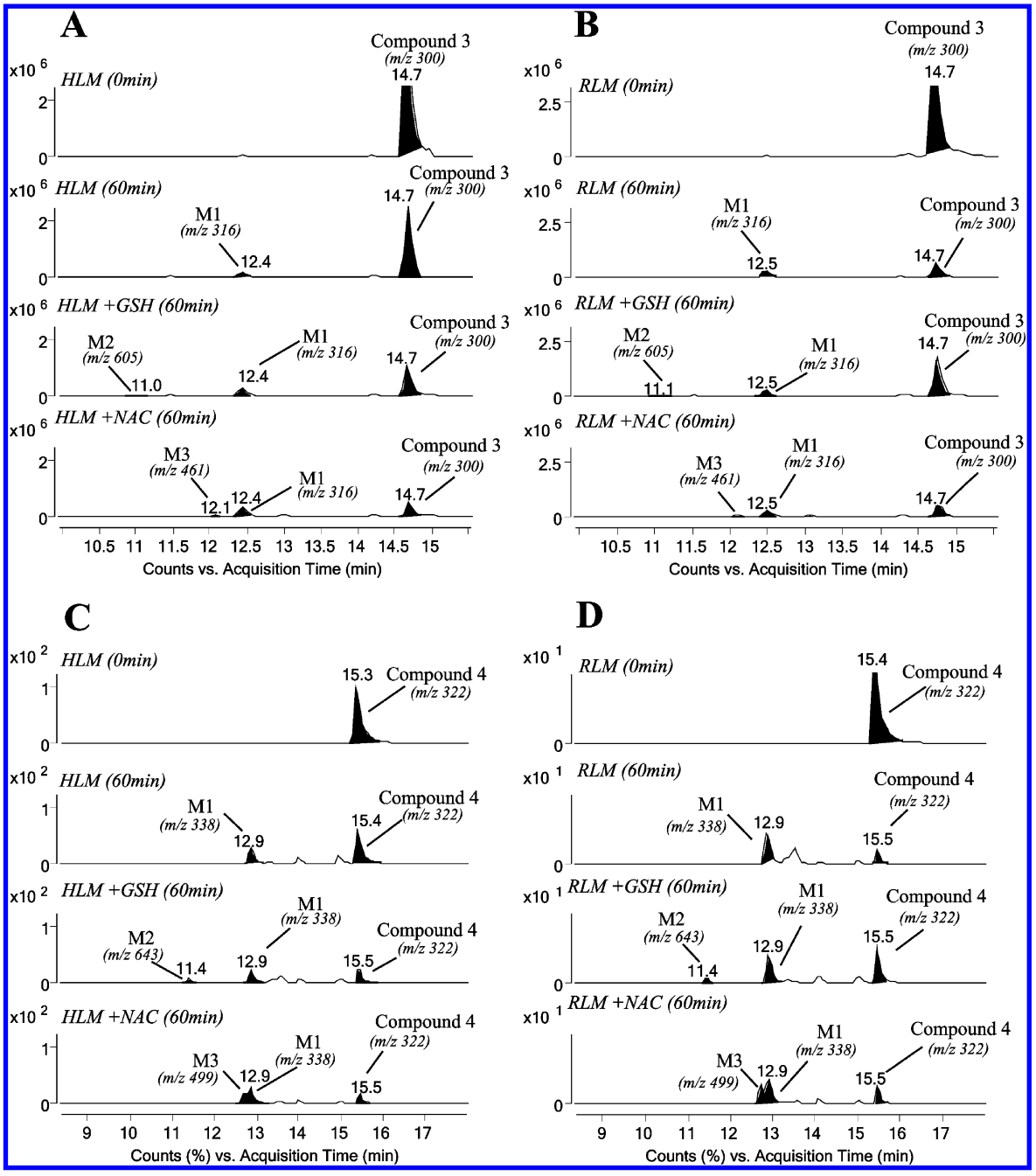


**Figure 3.** LC-MS base peak ion chromatograms for the parent and metabolites. (A) Metabolism of **3** in HLM and analysis of samples for BPC of *m/z* 300, 316, 461, and 605. (B) Metabolism of **3** in RLM and analysis of samples for BPC of *m/z* 300, 316, 461, and 605. (C) Metabolism of **4** in HLM and analysis of samples for BPC of *m/z* 322, 338, 499, and 643. (D) Metabolism of **4** in RLM and analysis of samples for BPC of *m/z* 322, 338, 499, and 643.

at *m/z* 595 $[M + H]^+$ (parent+323 Da) were observed in incubation samples supplemented with GSH for **1**. These peaks were not observed in the absence GSH, suggesting that these peaks were GSH adducts. Additionally, peaks (M4 and M5; Figure 1C) correlating to NAC adducts were seen at *m/z* 451 $[M + H]^+$ (parent + 179 Da) in incubations containing NAC, and these peaks were not observed in the absence of NAC. To further examine the nature of GSH or NAC conjugates, HDMS experiments (Figure S1.B, Supporting Information) were performed revealing the presence of 10 exchangeable protons in GSH conjugates at *m/z* 606 $[M + D]^+$ (6 accounted for GSH plus 3 accounted for compound and one from hydroxyl group) and 6 exchangeable protons in NAC conjugates at *m/z* 458 $[M + D]^+$ (2 from NAC plus 3 accounted for the compound and one from the hydroxyl group). Therefore, the metabolites M2 and M3 were characterized as dihydrohydroxy GSH adducts, and M4 and M5 were characterized as dihydrohydroxy NAC adducts. This observation was further corroborated by the chemical formula derived by HRMS for these metabolites. The putative GSH and NAC adducts were not quantified owing to the low abundance in the incubation mixtures (adducts were detected only by LC-MS, and no adduct peaks were detected in UV chromatograms).


dx.doi.org/10.1021/tx500212c | *Chem. Res. Toxicol.* XXXX, XXX, XXX−XXX

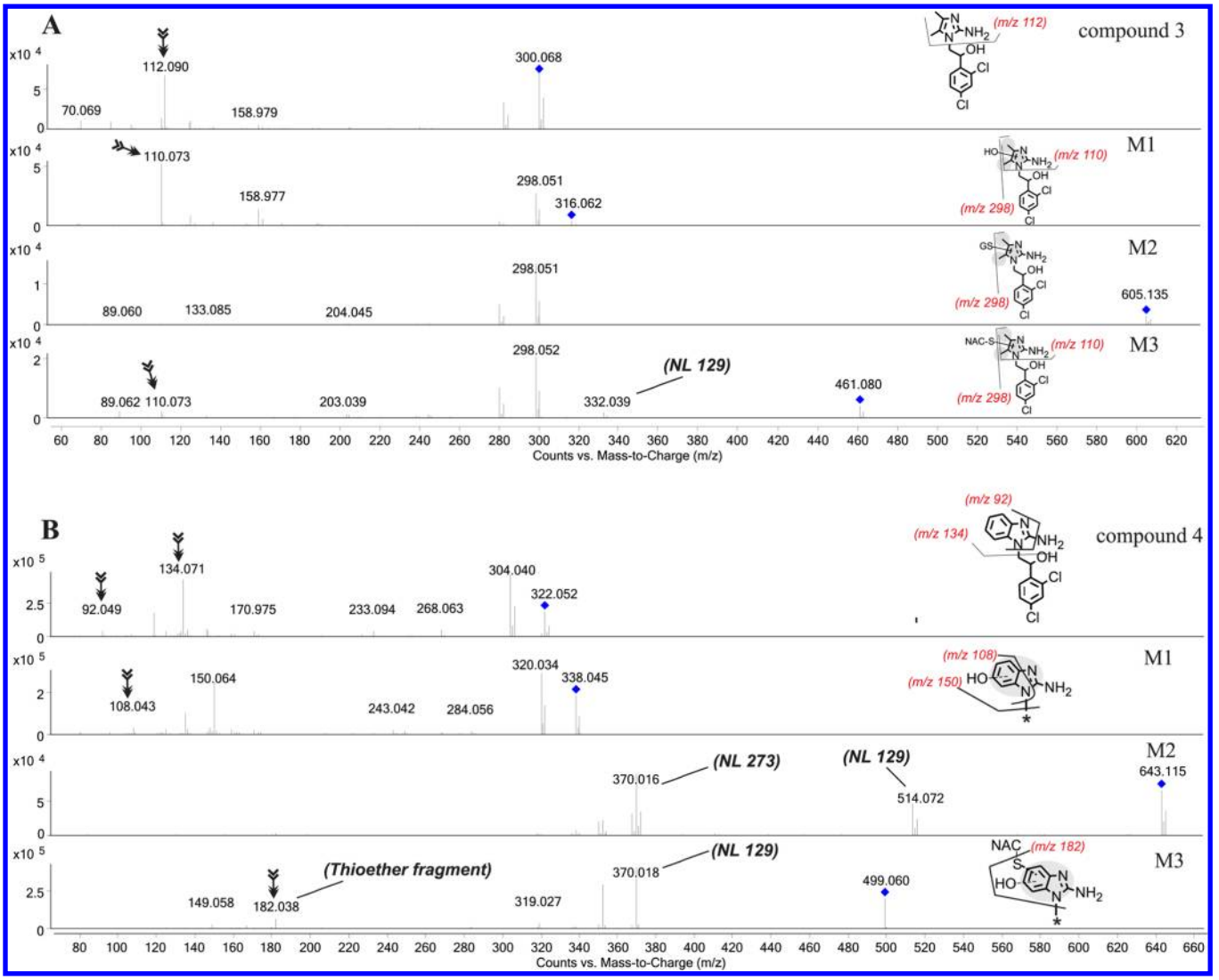


**Figure 4.** MS2 spectra of (A) **3** and its metabolites, and (B) **4** and its metabolites.

Figure 1D shows the chromatograms for GSH or NAC supplemented RLM/HLM incubations of **2**. Similar to **1**, dihydrohydroxy GSH (parent + 323 Da) and NAC adducts (parent + 179 Da) were also observed for **2**. These adducts had ion peaks at $m/z$ 575 $[M + H]^+$ (M3 and M4) and 431 $[M + H]^+$ (M5 and M6). In HDMS analysis, these metabolites formed ions at $m/z$ 586 $[M + D]^+$ (M3 and M4) and 438 $[M + D]^+$ (M5 and M6) (Figure S2.B, Supporting Information) indicating a process similar to that observed for **1**.

When **1** and **2** were preincubated with ABT (1 mM) in RLM/HLM and GSH or NAC incubations, the formation of all the metabolites of **1** and **2** was inhibited (data not shown).

**Effect of Blocking of C4 and C5 of Imidazole on RM Formation.** When **3** ($m/z$ 300 $[M + H]^+$; Table 1) was incubated with HLM (Figure 3A) and RLM (Figure 3B), only one oxidative metabolite (M1, $m/z$ 316 $[M + H]^+$) was produced after 60 min of incubation in the presence of NADPH, without other added cofactors. MS2 spectra of M1 (Figure 4A) showed a fragment at $m/z$ 110 indicative of the loss of water, and suggested the hydroxylation of the $CH_3$ group in the imidazole part of the molecule. In GSH supplemented incubations (Figure 3A and B), an additional peak M2 was seen at $m/z$ 605 $[M + H]^+$ (parent + 305 Da), whereas incubations containing NAC (Figure 3A and B) produced one additional peak M3 at $m/z$ 461 $[M + H]^+$ (parent + 161 Da). The chemical formula derived from HRMS data for M2 and M3 indicated the addition of GSH (305 Da) and NAC (161 Da) to **3**, respectively. The characteristic fragment at $m/z$ 112 corresponding to 4,5-dimethy-2-amino-imidazole portion of **3** (Figure 4A) was not observed for both M2 and M3 (Figure 4A). Moreover, MS2 spectra of M3 contained a peak at $m/z$ 110 suggestive of neutral loss of the NAC moiety[14,15] from the 4,5-dimethyl-2-aminoimidazole portion of the molecule.

Similarly, **4** underwent metabolism in HLMs (Figure 3C) and RLMs (Figure 3D) to form a single hydroxyl metabolite M1 ($m/z$ 338 $[M + H]^+$). The characteristic fragments (Figure 4B) at $m/z$ 134 and 92, corresponding to the benzimidazole moiety of the parent, were not observed for M1. Instead, fragments at $m/z$ 150 (134 + 16 Da) and 108 (92 + 16 Da) were seen, suggesting hydroxylation at benzimidazole moiety on **4**. An additional peak M2 was identified in GSH supplemented incubations at $m/z$ 643 $[M + H]^+$. The mass of M2 correlated to the GSH conjugate of hydroxyl metabolite (parent + 16 + 305 Da) of **4**. Similarly, the NAC conjugate peak (M3) was observed at $m/z$ of 499 $[M + H]^+$ (parent + 16


dx.doi.org/10.1021/tx500212c | Chem. Res. Toxicol. XXXX, XXX, XXX−XXX

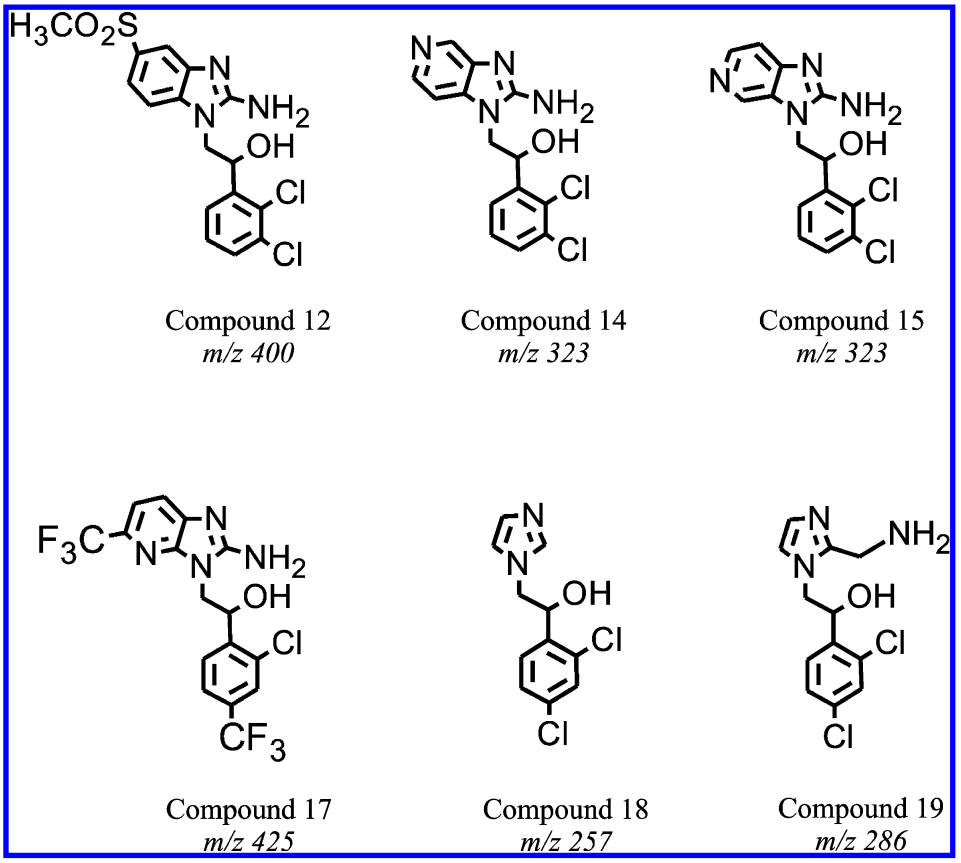


**Figure 5.** Chemical structures of compounds which do not undergo RM formation.

+ 161 Da) in NAC supplemented incubations (Figure 3C and D). MS2 spectra of M2 and M3 hinted toward the metabolism in the benzimidazole moiety (Figure 4B) since the fragment at *m/z* 134 was not observed for both the metabolites. Rather a fragment ion at *m/z* 182 (134 + 16 + 32 Da) was observed for M3, indicating the addition of -OH and -SH to the benzimidazole part (Figure 4B). Both M2 and M3 presented a fragment at *m/z* 370, attributed to characteristic neutral loss of 129 amu from NAC conjugates[14,15] and of 273 amu from GSH adducts.[15] A fragment ion peak at *m/z* 514 corresponding to the NL of 129 amu from GSH was also observed for M2 (*m/z* 643) (Figure 4B).

**Effect of Structural Modification of the Benzimidazole Ring on RM Formation.** To investigate the effect of structural modification on the metabolic activation, a variety of aminobenzimidazole derivatives were selected for testing (Table 1 and Figure 5). These are categorized as benzimidazole derivatives (**5** to **12**) and azabenzimidazole derivatives (**13** to **17**). In vitro assays were performed with each test compound with RLMs in the presence of GSH or NAC. As shown in Table 1, compounds **5**−**11**, **13**, and **16** showed the formation of GSH and NAC adducts in incubations with RLMs and HLMs, which were supplemented with GSH and NAC, respectively. The observed fragmentation patterns for NAC adducts for each of these compounds suggests that the adduct formation appears to be occurring at the benzimidazole ring (Figure S3−S7, Supporting Information). In addition, all compounds showed the presence of a CYP-mediated metabolite (Table 1). In contrast, compounds **12**, **14**, **15**, and **17** (Figure 5) did not show formation of GSH or NAC adducts.

**Effect of Modification of Imidazole $NH_2$ on RM Formation.** Effect of modification, substitution, or removal of imidazole $NH_2$ on RM formation was studied in RLMs in the presence of NAC/GSH. No GSH or NAC adducts were formed in incubations with **18** and **19** (Figure 5).

## DISCUSSION

Drug bioactivation is believed to be responsible for some of the observed idiosyncratic adverse drug reactions.[9,16] In drug discovery, it is desirable to eliminate metabolic activation via structural modifications early in the process, thus mitigating potential risks in later clinical studies. Many reactive metabolites can form adducts with small molecule trapping agents.[17,18] Characterization of these adducts can provide indirect information on the structure of the reactive species from which they are derived, thereby providing an understanding of potential bioactivation mechanisms,[19] which in turn can lead to the elimination of reactive metabolites through rational drug design.

Dihydrodiol metabolites were observed during a routine in vitro metabolite identification study of **1** and **2** in HLMs and RLMs (Figure 1A and B). These metabolites, while nontoxic, are believed to be derived from a reactive epoxide intermediate.[20,21] Therefore, formation of these metabolites raises concern regarding potential bioactivation of the compound. We employed GSH and NAC as RM trapping agents in microsomal assays to confirm the metabolic activation of **1** and **2**. Routine RM trapping assays only involve GSH; however, we also used NAC to confirm our findings and help in structural characterization of adducts. Like GSH, NAC also contains a free sulfhydryl group that can react directly with soft


dx.doi.org/10.1021/tx500212c | *Chem. Res. Toxicol.* XXXX, XXX, XXX−XXX

**Scheme 1. Metabolism and Bioactivation of Compounds 1 (A) and 2 (B)**

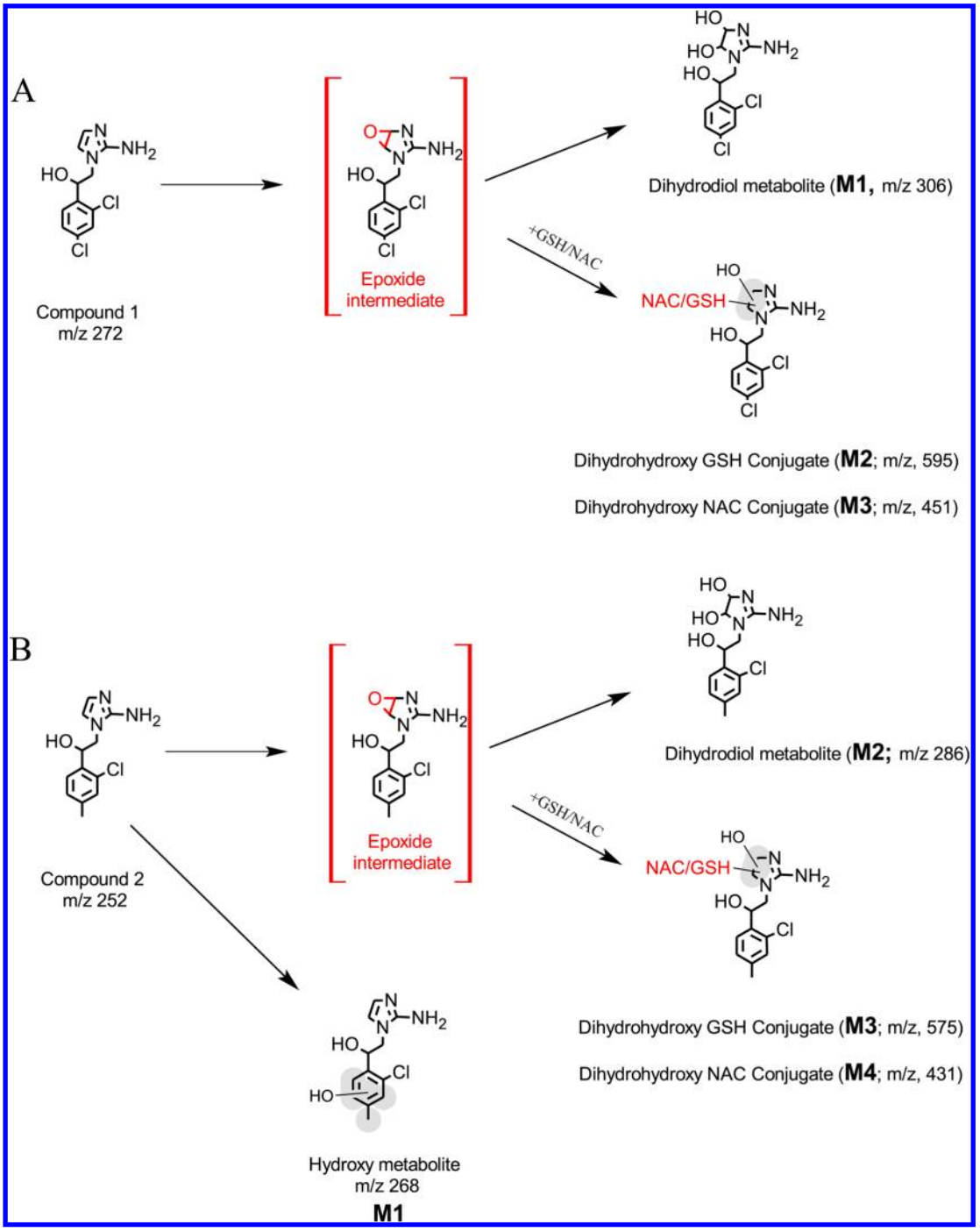


electrophiles, like quinones, epoxides, Michael acceptors, etc. to form stable thioether adducts.[18,22]

Two dihydrohydroxy GSH and NAC conjugates (Figure 1C and D) were observed for both compounds in the RM trapping assay. This provided direct evidence for the novel epoxidation pathway in imidazole metabolic activation (Scheme 1). Five membered heterocyclic rings like furans, thiophenes, and thiazoles have been found to undergo epoxidation,[23−25] and bioactivation of methyl imidazole to imidazomethide reactive intermediate has been reported previously;[26] however, the formation of epoxides on imidazole rings has not been previously reported. Therefore, this is the first report of an epoxide intermediate in metabolic activation of an imidazole ring.

Mitigation of epoxidation by methyl substitution has been reported in case of thiazole rings.[27] Therefore, a similar strategy was employed, and C-4 and C-5 of the imidazole ring were blocked by methyl substitution in **3** (Table 1). This strategy prevented epoxidation and the formation of subsequent dihydrohydroxy GSH or NAC adducts for **3**. However, bioactivation was still observed for this compound as direct GSH (M2) and NAC (M3) adducts with *m*/*z* parent + 305 Da and parent + 161 Da were detected in microsomal incubations (Figure 3A and B), presumably formed via a putative imine-methide reactive intermediate (Scheme 2A). The precursor of


dx.doi.org/10.1021/tx500212c | *Chem. Res. Toxicol.* XXXX, XXX, XXX−XXX

**Scheme 2. Metabolism and Bioactivation of (A) Compounds 3 and (B) 4**

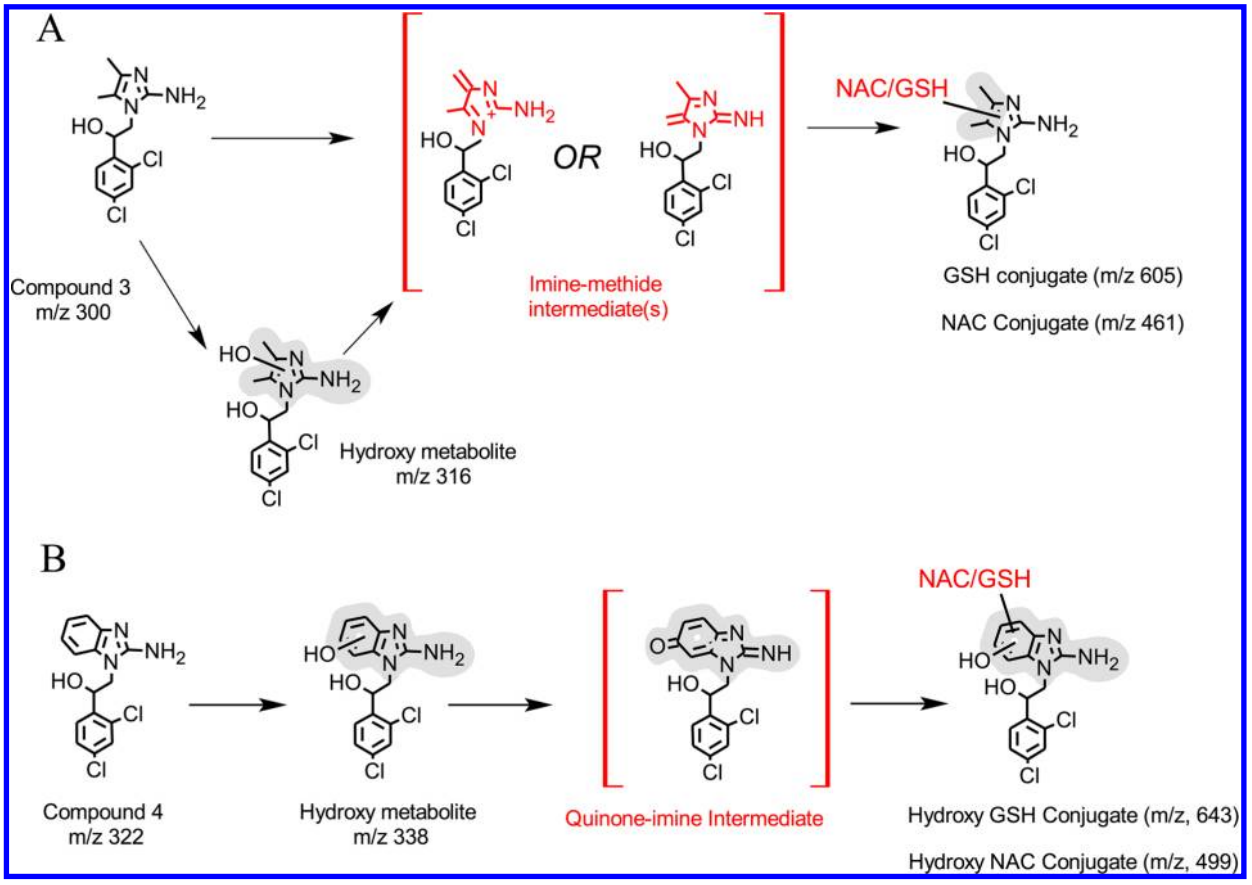


these GSH and NAC conjugates can be theoretically derived from the oxidation of compound **3** by formation of an imine methide reactive intermediate (Scheme 2A).

Masking the site of imidazole metabolism via benzimidazole, **4**, blocked the imine-methide formation; however, **4** produced hydroxy GSH (M2) and hydroxy NAC adducts (M3) (Figure 3C and D) suggesting the possible formation of quinone-imine intermediates (Scheme 2B). Formation of quinone-imine intermediate in the case of benzimidazoles is not surprising, as the embedded ortho arrangement of the two imidazole nitrogen atoms could contribute toward the high electron density in the phenyl ring leading to oxidation and subsequent two electron abstraction to form reactive *ortho*- and *para*-quinone imine intermediates[28] (Scheme 2B).

To eliminate the possible involvement of the dichloro-phenyl part of the molecule in RM formation and to further confirm the bioactivation of benzimidazole ring, a structural analogue was synthesized wherein the phenyl ring (**4**) was replaced by a pyridine ring (**5**) (Table 1). As expected, **5** showed the same trend and formed hydroxy GSH and NAC conjugates (Figure S3, Supporting Information, and Scheme 3, A).

In order to block hydroxylation and subsequent quinone-imine formation, by reducing the electron density and deactivating the benzimidazole ring, a −CF3 group was introduced ortho to the unsubstituted imidazole nitrogen (**6**; Table 1). However, this approach did not mitigate quinone-imine formation as hydroxylation and hydroxy GSH and NAC conjugation were observed (Figure S4, Supporting Information, and Scheme 3, B), suggesting that the orthro position is probably not the main soft spot or that the metabolism has switched to another position.

Fluorine substitution at the meta position (**7**; Table 1) and para position (**8**; Table 1) of unsubstituted imidazole nitrogen was studied in order to understand the effect on bioactivation of benzimidazole. Both compounds showed the formation of defluoro-hydroxy GSH and NAC conjugates via putative quinone-imine intermediates (Figures S5A and S5B, Supporting Information). However, the mechanism of adduct formation appears to be different for the two compounds. It is proposed that **8** first undergoes oxidative defluorination leading to the formation of a quinine imine that subsequently forms defluorinated thioether conjugates when incubated in the presence of GSH or NAC (Scheme 3, D), whereas hydroxylation of **7** leads to the formation of a quinone-imine intermediate that finally results in defluorinated GSH or NAC conjugates via nucleophilic substitution of fluorine (Scheme 3, C). This observation highlighted the vulnerability of the para position for oxidation and subsequent quinone-imine formation. Fluorinated aromatic compounds are generally resistant to metabolism. However, metabolic defluorination catalyzed by cytochrome P450[29] or FMO[30] enzymes has been reported, which could be attributed to the fluoride ion being a good leaving group in the substitution reaction.

Cyano substitutions at the meta position (**9**) resulted in hydroxy GSH or NAC conjugates (Figure S6A, Supporting Information, and Scheme 3, E), whereas cyano substitution at the para position (**10**) resulted in descyano hydroxy GSH and NAC conjugates (Figure S6B, Supporting Information, and Scheme 3, F), further highlighting the vulnerability of para carbon for enzymatic oxidation. We propose that **10** first undergoes oxidative denitrilation leading to the formation of a quinine imine intermediate that subsequently forms descyano


dx.doi.org/10.1021/tx500212c | *Chem. Res. Toxicol.* XXXX, XXX, XXX−XXX

**Scheme 3. Effect of Structural Modification on RM Formation (Compounds 5 to 12)**[a]

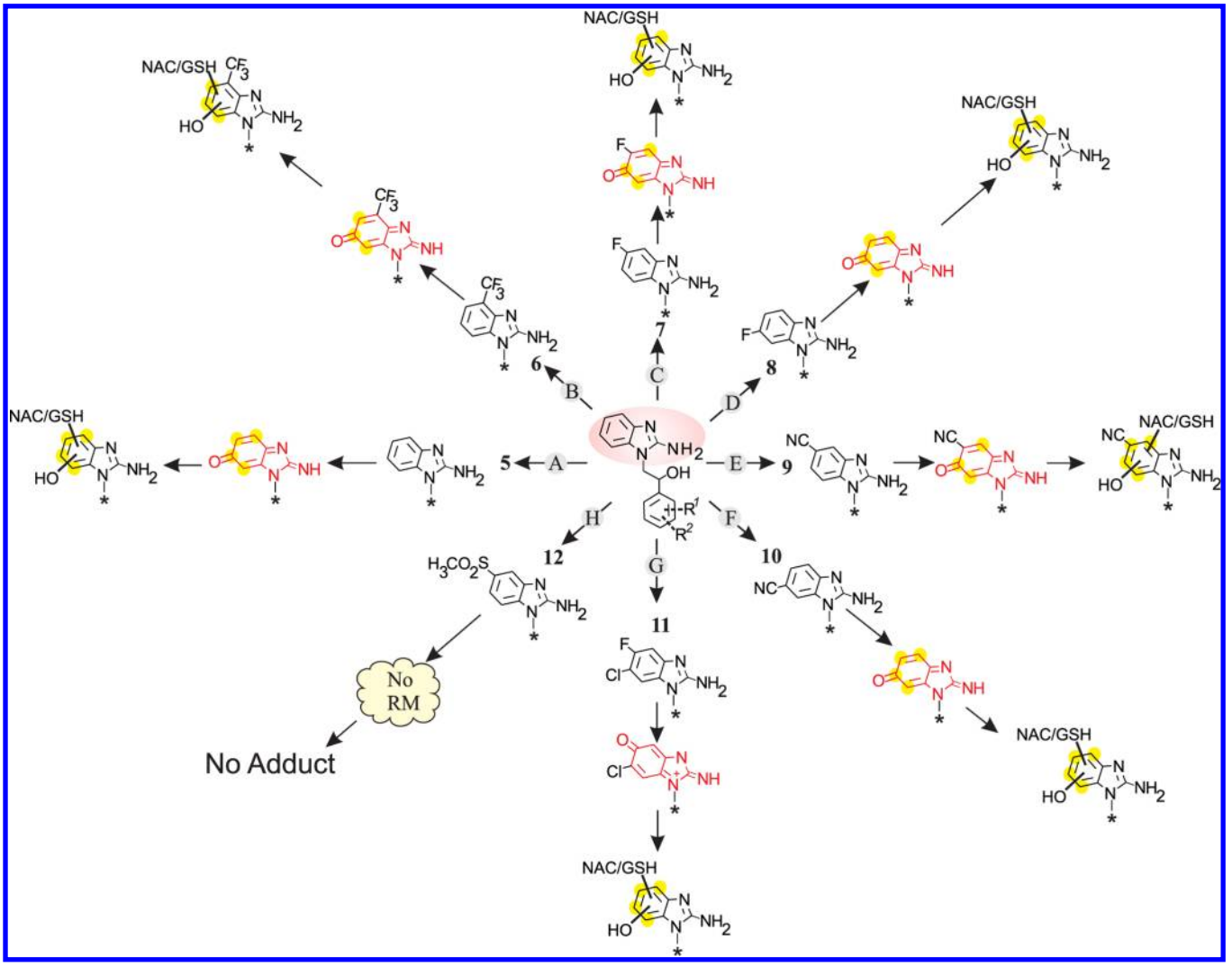


[a]Representative structures of proposed RM and thioether adducts are shown.

hydroxy GSH and NAC conjugates (Scheme 3, F), whereas **9** undergoes hydroxylation to form quinone-imine intermediates (Scheme 3, E). Bioactivation of **11** resulted in defluoro-dechloro hydroxy GSH or NAC conjugate (Figure S5C, Supporting Information, and Scheme 3, G). The only benzimidazole compound which was not found to undergo bioactivation was a methyl sulfone analogue (**12**; Figure 5). In addition to being a strong electrophile, methyl sulfone is also a bulky group which can sterically obstruct the enzymatic attack on metabolically vulnerable benzimidazole ring carbons (Scheme 3, H).

Further, we studied the effect of the inclusion of nitrogen at different positions of benzimidazole on RM formation (Scheme 4). Incorporation of nitrogen decreases the electron density in the aromatic ring carbons, thereby decreasing P450 mediated aromatic oxidation.[31] It was observed that the presence of nitrogen at either of two ortho postions to the imidazole ring (**13** and **16**; Table 1) does not have any impact on bioactivation (Scheme 4A and D) (Figure S7, Supporting Information), whereas **14** and **15** (Figure 5) which have nitrogen at the meta and para positions to unsubstituted imidazole nitrogen, respectively, do not undergo bioactivation (Scheme 4B and C). The $CF_3$ substituted analogue (**17**; Figure 5) of **16**, however, did not form any thioether conjugate (Scheme 4E).

Removal of the -$NH_2$ group or substitution with the $-CH_2-NH_2$ group in imidazole ring (as in **18** and **19** respectively; Figure 5) mitigated RM formation thereby highlighting the importance of the lone pair of electrons on $-NH_2$ in the bioactivation of amino imidazoles.

As mentioned earlier, there were no attempts to quantitate the GSH adducts for the compounds reported here, and the testing reported in this article was used qualitatively to assess the risk of formation of reactive intermediates. Since reactive metabolites are linked with tissue binding and idiosyncratic toxicities, our efforts were focused on mitigating this risk by medicinal chemistry. Our goal was to identify molecules that did not show detectable levels of glutathione adducts by LC-MS, and here, we have successfully identified compounds that showed no adduct formation (Scheme 4).

In conclusion, this article throws light on a novel metabolic pathway and describes the effect of various structural modification strategies on RM formation/mitigation. Amino imidazole and benzimidazole rings are excellent structural motifs in medicinal chemistry as they offer favorable physicochemical properties to pharmacologically active mole-


dx.doi.org/10.1021/tx500212c | Chem. Res. Toxicol. XXXX, XXX, XXX−XXX

**Scheme 4. Effect of Structural Modification on RM Formation (compounds 13 to 17)[a]**

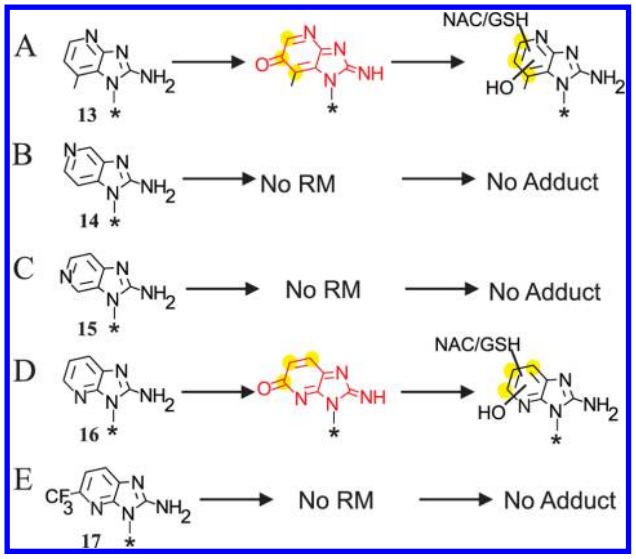


[a]Representative structures of proposed RM and thioether adducts are shown.

cules. Many compounds of therapeutic importance contain these motifs and thereby have the potential to form the types of reactive intermediates demonstrated here. By applying an understanding of drug metabolism and bioactivation, we have shown that it is possible to avoid the potential liability associated with aminoimidazoles and benzimidazoles.

## ■ ASSOCIATED CONTENT

### Supporting Information

Results of the HRMS experiments for compounds **1** and **2**, and MS2 spectra of the parent and metabolites for compounds **5**–**11**, **13**, and **16**. This material is available free of charge via the Internet at http://pubs.acs.org.

## ■ AUTHOR INFORMATION

### Corresponding Author

*Tel: +1 781-386-7725. E-mail: vinayak.hosagrahara@astrazeneca.com.

### Funding

This project was funded by Medicines for Malaria Venture (MMV 09/5400).

### Notes

The authors declare no competing financial interest.

## ■ ACKNOWLEDGMENTS

We thank Medicines for Malaria Venture (MMV) for their financial support of this project (MMV 09/5400). We give special thanks to Professor Steve Ward, Dr. David Waterson, and Dr. Simon Campbell for their scientific advice during the course of this project. Our heartfelt thanks go to Dr. Vasan Sambandamurthy, Dr. Pravin Iyer, and Dr. Shridhar Narayanan for their valuable input and support during this study. The authors are indebted to Chinnapattu Murugan, Praveena Manjrekar, Gajanan Shanbhag, and Krishna Koushik for synthesizing the compound used in this study and Dr. Prabhakar KR for technical input during the LC-MS analysis.

## ■ ABBREVIATIONS

GSH, glutathione; HLMs, human liver microsomes; HRMS, high resolution mass spectrometry; LC-MS, liquid chromatography–mass spectrometry; LC-MS/MS, liquid chromatography–tandem mass spectrometry; MS, mass spectrometry; MS2, tandem mass spectrometry; NAC, *N*-acetylcysteine; RLMs, rat liver microsomes; RM, reactive metabolite

## ■ REFERENCES

(1) Kola, I., and Landis, J. (2004) Can the pharmaceutical industry reduce attrition rates? *Nat. Rev. Drug Discovery 3*, 711–716.
(2) Lasser, K. E., Allen, P. D., Woolhandler, S. J., Himmelstein, D. U., Wolfe, S. M., and Bor, D. H. (2002) Timing of new black box warnings and withdrawals for prescription medications. *JAMA 287*, 2215–2220.
(3) Uetrecht, J. (2008) Idiosyncratic drug reactions: past, present, and future. *Chem. Res. Toxicol. 21*, 84–92.
(4) Smith, D. A., and Obach, R. S. (2006) Metabolites and safety: what are the concerns, and how should we address them? *Chem. Res. Toxicol. 19*, 1570–1579.
(5) Uetrecht, J. (2006) Evaluation of which reactive metabolite, if any, is responsible for a specific idiosyncratic reaction. *Drug Metab. Rev. 38*, 745–753.
(6) Guengerich, F. P. (2006) Cytochrome P450s and other enzymes in drug metabolism and toxicity. *AAPS J. 8*, E101–E111.
(7) Park, B. K., Kitteringham, N. R., Maggs, J. L., Pirmohamed, M., and Williams, D. P. (2005) The role of metabolic activation in drug-induced hepatotoxicity. *Annu. Rev. Pharmacol. Toxicol. 45*, 177–202.
(8) Park, B. K., Boobis, A., Clarke, S., Goldring, C. E., Jones, D., Kenna, J. G., Lambert, C., Laverty, H. G., Naisbitt, D. J., Nelson, S., Nicoll-Griffith, D. A., Obach, R. S., Routledge, P., Smith, D. A., Tweedie, D. J., Vermeulen, N., Williams, D. P., Wilson, I. D., and Baillie, T. A. (2011) Managing the challenge of chemically reactive metabolites in drug development. *Nat. Rev. Drug Discovery 10*, 292–306.
(9) Stachulski, A. V., Baillie, T. A., Kevin Park, B., Scott Obach, R., Dalvie, D. K., Williams, D. P., Srivastava, A., Regan, S. L., Antoine, D. J., Goldring, C. E. P., Chia, A. J. L., Kitteringham, N. R., Randle, L. E., Callan, H., Castrejon, J. L., Farrell, J., Naisbitt, D. J., and Lennard, M. S. (2013) The generation, detection, and effects of reactive drug metabolites. *Med. Res. Rev. 33*, 985–1080.
(10) Zhang, L., Peng, X. M., Damu, G. L. V., Geng, R. X., and Zhou, C. H. (2014) Comprehensive review in current developments of imidazole-based medicinal chemistry. *Med. Res. Rev. 34*, 340–437.
(11) Boiani, M., and Gonzalez, M. (2005) Imidazole and benzimidazole derivatives as chemotherapeutic agents. *Mini. Rev. Med. Chem. 5*, 409–424.
(12) El Rashedy, A. A., and Aboul-Enein, H. Y. (2013) Benzimidazole derivatives as potential anticancer agents. *Mini. Rev. Med. Chem. 13*, 399–407.
(13) Hosagrahara, V., Reddy, J., Ganguly, S., Panduga, V., Ahuja, V., Parab, M., and Giridhar, J. (2013) Effect of repeated dosing on rifampin exposure in BALB/c mice. *Eur. J. Pharm. Sci. 49*, 33–38.
(14) Scholz, K., Dekant, W., Volkel, W., and Pahler, A. (2005) Rapid detection and identification of N-acetyl-L-cysteine thioethers using constant neutral loss and theoretical multiple reaction monitoring combined with enhanced product-ion scans on a linear ion trap mass spectrometer. *J. Am. Soc. Mass Spectrom. 16*, 1976–1984.
(15) Srivastava, A., Lian, L. Y., Maggs, J. L., Chaponda, M., Pirmohamed, M., Williams, D. P., and Park, B. K. (2010) Quantifying the metabolic activation of nevirapine in patients by integrated applications of NMR and mass spectrometries. *Drug Metab. Dispos. 38*, 122–132.
(16) Srivastava, A., Maggs, J. L., Antoine, D. J., Williams, D. P., Smith, D. A., and Park, B. K. (2010) Role of Reactive Metabolites in Drug-Induced Hepatotoxicity, in *Adverse Drug Reactions* (Uetrecht, J., Ed.) pp 165–194, Springer, Berlin, Germany.
(17) Argoti, D., Liang, L., Conteh, A., Chen, L., Bershas, D., Yu, C. P., Vouros, P., and Yang, E. (2005) Cyanide trapping of iminium ion

reactive intermediates followed by detection and structure identification using liquid chromatography-tandem mass spectrometry (LC-MS/MS). *Chem. Res. Toxicol. 18*, 1537−1544.
(18) Evans, D. C., Watt, A. P., Nicoll-Griffith, D. A., and Baillie, T. A. (2004) Drug-protein adducts: an industry perspective on minimizing the potential for drug bioactivation in drug discovery and development. *Chem. Res. Toxicol. 17*, 3−16.
(19) Kalgutkar, A. S., and Soglia, J. R. (2005) Minimising the potential for metabolic activation in drug discovery. *Expert. Opin. Drug Metab. Toxicol. 1*, 91−142.
(20) Lau, S. S., Abrams, G. D., and Zannoni, V. G. (1980) Metabolic activation and detoxification of bromobenzene leading to cytotoxicity. *J. Pharmacol. Exp. Ther. 214*, 703−708.
(21) Zampaglione, N., Jollow, D. J., Mitchell, J. R., Stripp, B., Hamrick, M., and Gillette, J. R. (1973) Role of detoxifying enzymes in bromobenzene-induced liver necrosis. *J. Pharmacol. Exp. Ther. 187*, 218−227.
(22) Wen, B., and Fitch, W. L. (2009) Analytical strategies for the screening and evaluation of chemically reactive drug metabolites. *Expert Opin. Drug Metab. Toxicol. 5*, 39−55.
(23) Zhang, K. E., Naue, J. A., Arison, B., and Vyas, K. P. (1996) Microsomal metabolism of the 5-lipoxygenase inhibitor L-739,010: evidence for furan bioactivation. *Chem. Res. Toxicol. 9*, 547−554.
(24) Dansette, P. M., Bertho, G., and Mansuy, D. (2005) First evidence that cytochrome P450 may catalyze both S-oxidation and epoxidation of thiophene derivatives. *Biochem. Biophys. Res. Commun. 338*, 450−455.
(25) Peterson, L. A. (2006) Electrophilic intermediates produced by bioactivation of Furan. *Drug Metab. Rev. 38*, 615−626.
(26) Hutzler, J. M., Steenwyk, R. C., Smith, E. B., Walker, G. S., and Wienkers, L. C. (2004) Mechanism-based inactivation of cytochrome P450 2D6 by 1-[(2-ethyl-4-methyl-1H-imidazol-5-yl)methyl]- 4-[4-(trifluoromethyl)-2-pyridinyl]piperazine: kinetic characterization and evidence for apoprotein adduction. *Chem. Res. Toxicol. 17*, 174−184.
(27) Obach, R. S., Kalgutkar, A. S., Ryder, T. F., and Walker, G. S. (2008) In vitro metabolism and covalent binding of enol-carboxamide derivatives and anti-inflammatory agents sudoxicam and meloxicam: insights into the hepatotoxicity of sudoxicam. *Chem. Res. Toxicol. 21*, 1890−1899.
(28) Bolton, J. L., Trush, M. A., Penning, T. M., Dryhurst, G., and Monks, T. J. (2000) Role of quinones in toxicology. *Chem. Res. Toxicol. 13*, 135−160.
(29) Li, X., Kamenecka, T. M., and Cameron, M. D. (2009) Bioactivation of the epidermal growth factor receptor inhibitor gefitinib: implications for pulmonary and hepatic toxicities. *Chem. Res. Toxicol. 22*, 1736−1742.
(30) Driscoll, J. P., Aliagas, I., Harris, J. J., Halladay, J. S., Khatib-Shahidi, S., Deese, A., Segraves, N., and Khojasteh-Bakht, S. C. (2010) Formation of a quinoneimine intermediate of 4-fluoro-N-methylaniline by FMO1: carbon oxidation plus defluorination. *Chem. Res. Toxicol. 23*, 861−863.
(31) Dalvie, D., Kang, P., Loi, C. M., Goulet, L., and Nair, S. (2010) Chapter 7 Influence of Heteroaromatic Rings on ADME Properties of Drugs, in *Metabolism, Pharmacokinetics and Toxicity of Functional Groups: Impact of Chemical Building Blocks on ADMET*, pp 328−369, The Royal Society of Chemistry, Cambridge, U.K.